^{133}Cs nuclear magnetic resonance study of one-dimensional fluctuations in CsH_2PO_4 and its ferroelectric and antiferroelectric transitions at high pressure

Paul J. Schuele* and V. Hugo Schmidt
Physics Department, Montana State University, Bozeman, Montana 59717
(Received 29 August 1988)

Pressure and temperature effects on the one dimensional (1D) and higher-dimensionality correlations associated with the ferroelectric and antiferroelectric phase transitions in cesium dihydrogen phosphate were studied by means of the ^{133}Cs nuclear magnetic resonance (NMR) spin-lattice relaxation time T_1. We measured T_1 at 6.5 MHz at temperatures down to the ferroelectric (FE) Curie point T_C at 1 bar and at 1.5 and 3.0 kbar, down to the triple point $T_t = 124.6$ K at 3.3 kbar, and down to the antiferroelectric (AFE) Néel point T_N at 3.6 kbar. With decreasing temperature, T_1 first decreases exponentially due to 1D fluctuations associated with the J_b interactions in disordered hydrogen-bonded chains running along b. As the temperature falls further, T_1 then decreases linearly as the J_c interaction between these chains in hydrogen-bonded planes comes into play. From these results and the known pressure derivatives of T_C and T_N, we calculated pressure dependences for J_b, J_c, and for the interplanar interaction J_a. At 3.3 kbar J_a changes sign, so the plane stacking becomes AFE instead of FE. Above 8.9 kbar, where J_c extrapolates to zero, a new AFE phase with a checkerboard arrangement of FE b chains is predicted.

I. INTRODUCTION

Cesium dihydrogen phosphate (CDP) is a hydrogen-bonded crystal with highly anisotropic interactions which lead to strong one-dimensional correlations over a wide temperature range above its phase transition temperature. It is paraelectric (PE) at room temperature and undergoes a ferroelectric (FE) phase transition at 153 K.[1] In addition, dielectric[2] and neutron-diffraction measurements[3] at high pressure have revealed a third antiferroelectric (AFE) phase at pressures above 3.3 kbar and temperatures less than 125 K.

In the paraelectric phase CDP is monoclinic ($P2_1/m$) with two formula units per unit cell. Cesium atoms and PO_4 groups are centered on mirror planes perpendicular to the b axis at the fractional coordinates $y = \frac{1}{4}$ and $\frac{3}{4}$. Phosphate groups are linked together by hydrogen bonds of two inequivalent types; hydrogens in bonds approximately parallel to the c axis are ordered at off-center sites in the hydrogen bond, while hydrogens linking phosphate groups in zig-zag chains along the b axis are positionally disordered in double-minimum potential wells. Thus PO_4 groups are linked by a square network of hydrogen bonds producing a series of b-c planes separated by cesium atoms. In the ferroelectric phase b-chain hydrogens[4] order in one of the two off-center sites in the O—H $\cdots$ O bonds while the positions of hydrogens in c axis H bonds are unaffected. This hydrogen ordering is accompanied by a shift of Cs^+ and PO_4^{3-} groups along the b axis which yields a spontaneous polarization along b. In the pressure-induced AFE phase the structure doubles along the a axis due to antiferroelectric stacking of FE ordered b-c planes.[3] This AFE phase structure has also been observed for CsD_2PO_4.[5]

Neutron-diffraction experiments[5,6] have shown strong quasielastic scattering in narrow reciprocal space planes perpendicular to the ferroelectric b axis on approaching T_C. This shows that the correlations associated with ferroelectric ordering are strongly one dimensional along the b-axis hydrogen bonds. The interactions between adjacent b-axis chains linked by c-axis hydrogen bonds are weaker by about a factor of 100 and correlations in the a direction are weaker still. Also, correlations along a and c decrease rapidly with increasing temperature above T_C while the b-axis correlations are apparent as much as 50 K above T_C.

In addition to the neutron-scattering experiments,[5,6] evidence for long-range correlations has been observed in dielectric susceptibility,[7,8] electron paramagnetic resonance (EPR),[9] and nuclear magnetic resonance[10–15] (NMR) experiments. The NMR work includes ^{31}P, ^{17}O, deuteron, and ^{133}Cs resonance studies.

This report begins with a description of our apparatus and experimental method, continues with presentation of experimental results and their analysis, and concludes with a discussion of the results including a prediction of a new AFE phase with checkerboard-chain ordering at pressures above 8.9 kbar.

II. EXPERIMENT

The experimental arrangement consists of a Varian electromagnet having a 13-cm gap which accommodates a high-pressure, low-temperature apparatus described elsewhere.[16,17] Briefly, it consists of a beryllium-copper high-pressure vessel surrounded by an evacuated liquid-nitrogen-cooled dewar. The pressure vessel is surrounded by a copper thermal radiation shield, and both vessel and shield have separate heaters and temperature controls which provide long-term thermal stability of ± 2 mK. The high-pressure medium was helium gas which was pressurized as high as 3.6 kbar with long-term stability limited by a helium leak causing a pressure-loss rate of 2 bar/h at 3.6 kbar.

The sample was cut from an optically clear single crys-

tal grown by slow evaporation from an aqueous solution of Cs_2CO_3 and P_2O_5. It was mounted with the b axis parallel to the applied static magnetic field H_0 and the c axis parallel to the NMR field H_1. At this orientation the quadrupolar splitting collapses,[14] so the NMR response consists of a single Zeeman line with a well-defined spin-lattice relaxation time (T_1).

The NMR spectrometer was operated at a fixed frequency of 6.5 MHz which corresponds to a field of 1.1639 T for ^{133}Cs nuclei. To measure the spin-lattice relaxation time T_1, the spin system was first saturated by a comb of 90° pulses, and then after a waiting time τ the response to a 90° pulse was observed. The free induction decay after the pulse was digitized and the response amplitude I at a suitable delay after the end of the 40-μsec dead time was noted, and compared to the amplitude I_0 for long τ. A semilogarithmic plot of I_0-I against τ yielded straight lines, indicating a single relaxation time T_1.

Most of our T_1 measurements were made from 220 K down to 2° or 3° above the ferroelectric or antiferroelectric transition temperature, which ranged from 153 K at 1 bar to 123 K at 3.6 kbar. These measurements were made at five hydrostatic pressures, namely 1 bar and 1.5, 3.0, 3.3, and 3.6 kbar. The paraelectric-ferroelectric-antiferroelectric triple point occurs at 3.3 kbar and 124 K, approximately. Therefore, we were able to observe the behavior when approaching both the ferroelectric and antiferroelectric phases as well as when approaching the triple point.

The relaxation rate (T_1^{-1}) versus temperature (T) results are presented in Fig. 1 for the above pressures. To aid comparison, T_1 is plotted against T for all five pressures in Fig. 2. In general terms, at each pressure T_1 decreases with temperature in a similar way. At higher temperatures the T_1 behavior corresponds nearly to that expected for proton intrabond fluctuations in a strictly 1D Ising chain with FE coupling between protons. At lower temperature, T_1 exhibits a Curie-Weiss form extrapolating to zero T_1 at the ordering temperature for the 2D-coupled hydrogen-bonded planes. Detailed discussion of these phenomena and of the indirect evidence for a narrow third temperature regime dominated by the weak interplanar interaction is given in the following two sections.

III. THEORY

The interpretation of these results is made within the framework of a theory presented by Blinc, Ložar, Topič, and Žumer (abbreviated here as BLTZ).[15] In this theory the strongest interaction, which is the FE coupling in the ordering chains, is treated exactly. The intermediate-strength interaction between such chains within a hydrogen-bonded plane, and the weakest interaction which is between such planes, are treated in the mean-field approximation. We correct some misprints in the BLTZ equations. Also, we extend their mean-field analysis of the two weaker interactions, which they performed numerically without separating the effects of these two interactions, to show that the intermediate interaction causes Curie-Weiss–type dependence of T_1 on $T-T_{C\,2D}$, while the weakest interaction gives a dependence varying as $(T-T_C)^{1/2}$ in a narrow temperature range just above T_C.

The BLTZ theory has its roots in the wave-vector-dependent susceptibility for the pure 1D Ising model developed by Suzuki and Kubo,[18] and the static behavior including the phase transition for a system of weakly coupled 1D chains studied by Scalapino *et al.*[19] Žumer[20] combined those two approaches to obtain the $\hat{q}$-dependent susceptibility for the weakly coupled system. BLTZ introduced anisotropy into the interchain interactions and calculated quadrupolar spin-lattice relaxation from the ac dielectric susceptibility using the fluctuation-dissipation theorem. In each case, the intrachain interactions were treated exactly and the interchain interactions in the mean-field approximation.

The BLTZ theory begins with the assumption that the dominant mechanism for spin-lattice relaxation is the interaction of the nuclear electric quadrupole moment with the fluctuating electric field gradient (efg). This assumption appears to be correct over the temperature ranges covered in our experiments. It is further assumed that the quadrupolar interaction is small compared to the Zeeman interaction of the nuclear magnetic dipole moment with the applied magnetic field H_0. Under these assumptions the inverse spin-lattice relaxation time $1/T_1$ for quadrupolar relaxation of nuclei having spin I ($I=\frac{7}{2}$ for ^{133}Cs) and quadrupole moment Q is given by

$$\frac{1}{T_1}=\frac{e^4Q^2}{40\hbar^2}\frac{2I+3}{I^2(2I-1)}[J^{(1)}(\omega)+4J^{(2)}(2\omega)]\ , \tag{1}$$

in which the spectral density of the autocorrelation function for the fluctuating efg tensor at the ^{133}Cs site is

$$J^{(k)}(\omega)=\int_{-\infty}^{\infty}\langle V^{(k)}(0)V^{(-k)}(t)\rangle\exp(ik\omega t)dt\ . \tag{2}$$

Here the following notation is used in terms of efg components for a system with the z axis along the applied magnetic field H_0:

$$\begin{aligned} V^{(\pm1)}&=V_{xz}\pm iV_{yz}\ , \\ V^{(\pm2)}&=\tfrac{1}{2}(V_{xx}-V_{yy})\pm iV_{xy}\ . \end{aligned} \tag{3}$$

In Eqs. (1) and (2), the average efg components contribute nothing to the relaxation, so in Eq. (3) we need only the magnitudes of the fluctuations about these averages. These fluctuations result mostly from atomic displacements within a "source radius" of perhaps 5 Å around the Cs nucleus, caused by proton motions in the disordered chains. Each Cs nucleus is within 5 Å of two disordered H-bonded chains belonging to the same H-bonded plane. We assume that the fluctuation correlation length is greater than the source radius, so the efg at a given Cs nucleus at a given instant approximates its static value inside a FE domain. (From the neutron-scattering study of Frazer *et al.*,[21] this assumption is good over a wide temperature range for the intrachain b correlations, and from their Fig. 6 may be good for 5 or 10 K above T_C for the c correlations between chains in the same H-bonded plane.) Accordingly, we choose for the magnitude of the fluctuations half of the difference between the two efg's deter-

mined by Kanda and Fujimara[14] for the two FE domains in the FE phase. This assumption differs somewhat from that of BLTZ, who used the difference between the efg for one FE domain type and the efg for the PE phase.

In the BLTZ development, Eq. (2) is then Fourier transformed, the random phase approximation is made, and the shortness of the efg source radius is invoked so that $V_q^{(i)}=V_0^{(i)}$, which leads to

$$J^{(1)}(\omega)=(V_{xz}^2+V_{yz}^2)j(\omega)\ ,$$
$$J^{(2)}(2\omega)=[\tfrac{1}{4}(V_{xx}-V_{yy})^2+V_{xy}^2]j(2\omega)\ . \tag{4}$$

Here $j(\omega)$ is a sum over Fourier components, which following Topič *et al.*[12] is related to the imaginary part of the pseudo-one-dimensional Ising model wave-number-dependent susceptibility,

$$j(\omega)=\frac{1}{N}\sum_q j_q(\omega)=\frac{2T}{CN}\sum_q \chi''(\omega,q)\ . \tag{5}$$

Here C is the Curie-Weiss constant for the dielectric behavior, N is the number of mobile protons, q is the wave vector, and a factor of 2 missing in BLTZ is inserted.

The BLTZ analysis for the susceptibility follows that of

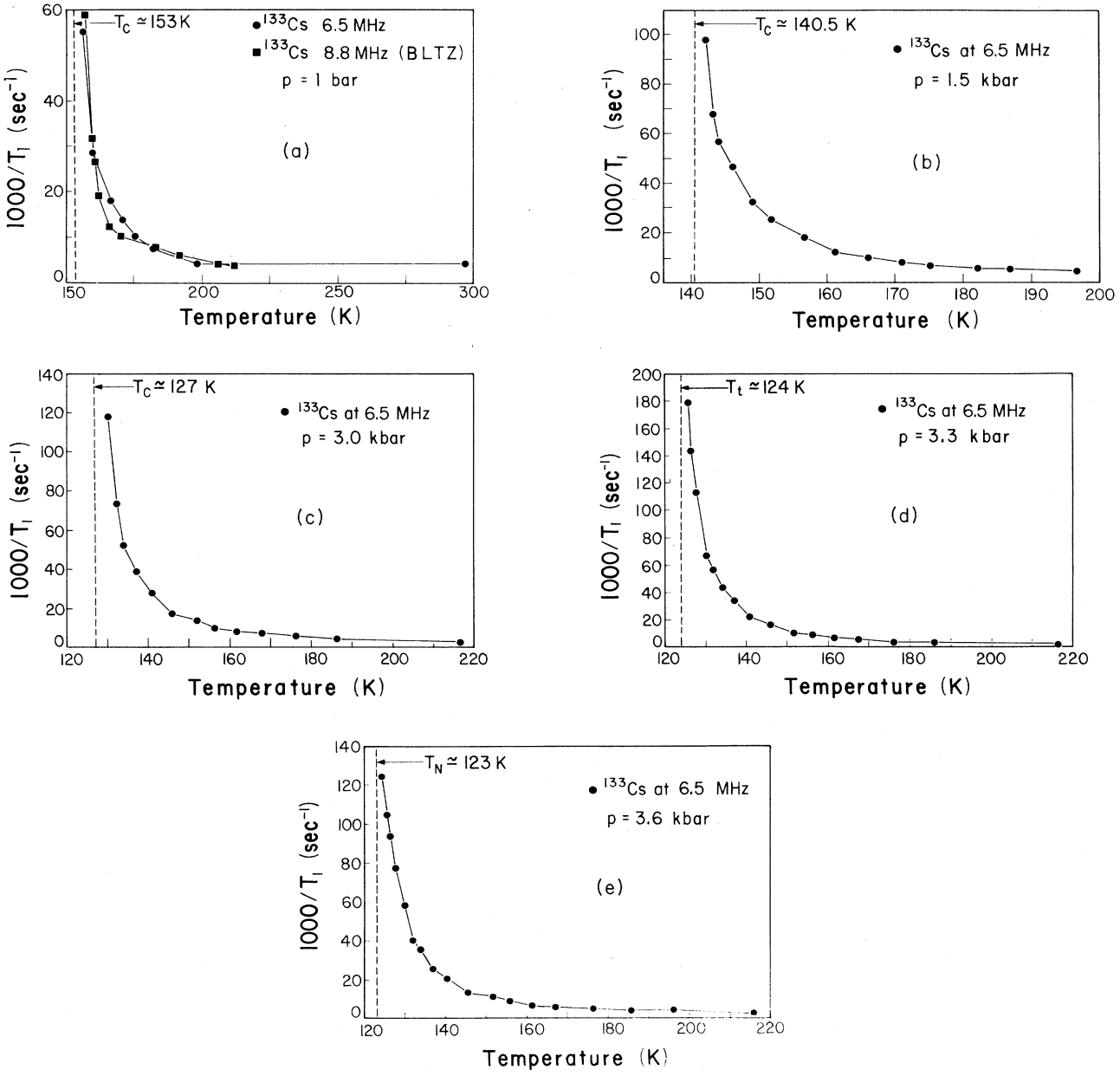

FIG. 1. Critical component of the spin-lattice relaxation rate for ^{133}Cs in CsH_2PO_4 as a function of temperature, at pressures of (a) 1 bar, (b) 1.5 kbar, (c) 3.0 kbar, (d) 3.3 kbar, and (e) 3.6 kbar.

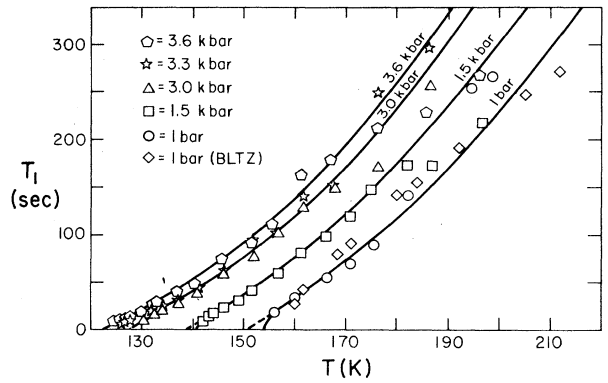

FIG. 2. Temperature dependence of the critical portion of ^{133}Cs spin-lattice relaxation time T_1 in CsH_2PO_4 for pressures of 1 bar, circles (BLTZ data shown by diamonds), 1.5 kbar (squares), 3 kbar (triangles), 3.3 kbar (stars), and 3.6 kbar (pentagons). Predictions of Eqs. (18) and (27) are indicated by solid lines. Dashed line portions correspond to an extrapolation of the 2D expression of Eq. (21). The line for 3.3 kbar is omitted for clarity.

Žumer,[20] ignoring tunneling which seems to have no major effect, treating intrachain interactions exactly via the one-dimensional Ising model, and treating the much weaker interchain interactions in the mean field. The Hamiltonian for the jth chain with z ($z=4$ for CDP) adjacent chains then is

$$H_j=-\sum_i\left[J_b p_{i+1,j}p_{i,j}+\sum_{m=1}^{z}J_{p,m}\langle p_{i,j+m}\rangle p_{i,j}\right], \quad (6)$$

where J_b is the $J_\parallel$ interaction for nearest proton neighbors in the disordered chains running along b, J_p is the $J_\perp$ interaction which is $(J_a+J_c)/2$ (nearly $J_c/2$ because $J_a \ll J_c$),[21] and the p's are pseudospins ±1 representing disordered proton positions.

From the susceptibility expression developed by BLTZ they obtain two expressions for $j(\omega)$ in their Eq. (26). The first is correct but the second should be

$$j(\omega)=\frac{2}{\pi^3}\tau_0 F\sin\gamma \times\int_0^\pi\int_0^\pi\int_0^\pi\frac{dx\,dy\,dz}{[D(x,y)-E\cos z]^2+(\omega\tau_0)^2}, \quad (7)$$

where D, E, F, and γ are defined below. We also define three new variables a, b, and f, which are more convenient for the following integrations:

$$D(x,y)=1-z'\beta J_p F(1+\alpha)^{-1}(\cos x+\alpha\cos y) =1-b(\cos x+\alpha\cos y), \quad \alpha=J_a/J_c\ll1, \quad (8)$$

$$E=\tanh(2\beta J_b)=1-a,\quad a=1-\tanh(2\beta J_b), \quad (9)$$

$$F=2\exp(-2\beta J_b),\quad f=\tau_0 F\sin\gamma, \quad \beta=1/kT,\quad T>T_C, \quad (10)$$

and γ is the monoclinic angle of 72.3°.

Upon integrating over z and neglecting $\omega\tau_0$ which is small for the frequency used in the temperature range studied, we obtain

$$j(\omega)=\frac{2}{\pi^2}\tau_0 F\sin\int_0^\pi\int_0^\pi\frac{D(x,y)dx\,dy}{[D^2(x,y)-E^2]^{3/2}}. \quad (11)$$

The $D(x,y)$ factor can be set to unity because $b\ll1$ for all $T>T_C$. The expression $[D^2(x,y)-E^2]$ can be broken into two subfactors,

$$D(x,y)-E=a-b(\cos x+\alpha\cos y), \quad (12)$$

$$D(x,y)+E=2-a-b(\cos x+\alpha\cos y)\simeq2-a, \quad (13)$$

using the fact that $(2-a)\gg b$ for all $T>T_C$. Then $j(\omega)$ becomes

$$j(\omega)\simeq\frac{2f}{\pi^2(2-a)^{3/2}}\int_0^\pi\int_0^\pi\frac{dx\,dy}{[a-b(\cos x+\alpha\cos y)]^{3/2}}. \quad (14)$$

Integration over x yields

$$j(\omega)\simeq\frac{4f}{\pi^2(2-a)^{3/2}}\times\int_0^\pi\frac{I[2b/(a-b-b\alpha\cos y)]}{(a-b-b\alpha\cos y)(a+b-b\alpha\cos y)^{1/2}}dy. \quad (15)$$

Here I represents a complete elliptic integral of the second kind. Both in the argument of I and in another factor,

$$(a+b-b\alpha\cos y)\simeq(a+b), \quad (16)$$

so the expression for $j(\omega)$ can be simplified to

$$j(\omega)\simeq\frac{4fI[2b/(a+b)]}{\pi^2(2-a)^{3/2}(a+b)^{1/2}}\int_0^\pi\frac{dy}{a-b-b\alpha\cos y}. \quad (17)$$

The final integration over y produces the expression

$$j(\omega)\simeq\frac{4fI[2b/(a+b)]}{\pi(2-a)^{3/2}[(a+b)(a-b+b\alpha)(a-b-b\alpha)]^{1/2}}. \quad (18)$$

This expression is valid over the entire temperature range above T_C within the approximations listed above. We now examine its predictions in four temperature regimes above T_C. These are the noncritical regime above room temperature, the 1D regime below room temperature but well above T_C, the 2D region extending to within a few degrees of T_C, and the 3D region in the last degree or two above T_C. We note that Morosov and Sigov[22] discussed the importance of the 1D, 2D, and 3D correlation regions for CsH_2PO_4 also, but in connection with dielectric permittivity.

In the noncritical regime the temperature is too high to allow correlations even of the protons in H-bonded chains running along b. In this regime, $1\gg(1-a)\gg b\gg\alpha b$, the argument of I approaches 0 so I approaches $\pi/2$, and Eq. (18) becomes

$$j(\omega)_{hi-T} \simeq 4\tau_0 \sin\gamma \ . \tag{19}$$

Here $kT \gg J_b \gg J_p \gg J_a$, and there is no significant temperature dependence predicted for $j(\omega)$ or for the spin-lattice relaxation rate T_1.

In the 1D regime we have $1 \gg a \gg b \gg \alpha b$, which yields

$$j(\omega)_{1D} \simeq \frac{2f}{(2a)^{3/2}} \simeq \tfrac{1}{2}\tau_0 \sin\gamma \exp(4\beta J_b) \ . \tag{20}$$

Physically this means that relaxation is governed by the Boltzmann factor for populations of (HPO_4,H_3PO_4) defect *pairs*. The effective diffusion of these defects by means of *b*-chain proton intrabond transfer causes the relaxation. As the temperature drops, the correlation time becomes longer because the defect population drops, and in the rapid-motion regime this increases the relaxation rate which is proportional to $j(\omega)$. The relaxation rate according to Eq. (20) would become infinite at absolute zero (the ordering temperature for the 1D Ising model), if Eq. (20) were valid down to that temperature.

In the 2D regime the inequality order becomes $1 \gg a \gg (a-b) \gg \alpha b$, so the argument of I, and I itself, approach 1 because $a + b \approx 2b$. Then $j(\omega)$ becomes

$$j(\omega)_{2D} \simeq \frac{f}{\pi b^{1/2}(a-b)} \ , \tag{21}$$

where the critical behavior is in the $(a-b)^{-1}$ factor which can be expanded to give the temperature dependence $(T - T_{C\,2D})^{-1}$. The Curie-Weiss temperature $T_{C\,2D}$ for this 2D regime is found from the implicit relation

$$2J_b/kT_{C\,2D} = -\ln[z'J_p/(1+\alpha)kT_{C\,2D}] \ . \tag{22}$$

This regime is recognized in the data by a straight portion of the T_1 versus T plot.

Before the temperature drops to $T_{C\,2D}$ the system goes over into the 3D regime characterized by $1 \gg a \gg (a - b + \alpha b) \gg (a - b - \alpha b)$. Then in addition to the approximations made in the 2D regime, we can also set $a - b + \alpha b \simeq 2\alpha b$, and we obtain

$$j(\omega) \simeq \frac{f}{\pi b[2a(a-b-\alpha b)]^{1/2}} \ . \tag{23}$$

The last factor when expanded gives critical temperature dependence $(T - T_C)^{-1/2}$, where T_C is the actual transition temperature which is slightly above $T_{C\,2D}$ and is given by the implicit relation

$$2J_b/kT_C = -\ln(z'J_p/kT_C) \ . \tag{24}$$

Because much of our T_1 data is in crossover regions between the above regimes, we use the general expression in Eq. (17) for $j(\omega)$. Since we are in the fast-motion regime, $j(\omega)$ actually has no dependence on frequency ω, so $j(2\omega) = j(\omega)$ in Eq. (4). Then the spectral density factor in Eq. (1) becomes

$$[J^{(1)}(\omega) + 4J^{(2)}(2\omega)] = [V_{xz}^2 + V_{yz}^2 + (V_{xx} - V_{yy})^2 + 4V_{xy}^2]j(\omega) \ . \tag{25}$$

According to Kanda and Fujimura,[14] the only efg tensor components at the ^{133}Cs site which change upon domain reversal in the FE phase of CDP are

$$\begin{aligned} eQV_{x'y'}/h &= eQV_{yz}/h = \pm 7.6 \text{ kHz} \ , \\ eQV_{y'z'}/h &= eQV_{xz}/h = \pm 12.5 \text{ kHz} \ , \end{aligned} \tag{26}$$

where the primed coordinates represent crystal axes and the unprimed coordinates represent laboratory system axes for our measurements in which the static magnetic field H_0 was along z, corresponding to the crystal y' or b axis.

From the discussion following Eq. (3), the above numbers divided by eQ/h are squared to provide V_{xz}^2 and V_{yz}^2 in Eq. (25), and the other V_{ij} in that equation vanish. Then, using $I = \frac{7}{2}$ for ^{133}Cs, Eq. (1) becomes

$$1/T_1 = 2.87 \times 10^7 s^{-2} j(\omega) \ . \tag{27}$$

Although we do not use Eqs. (28)–(33) of BLTZ, it is helpful for anyone using that approach to note the following corrections. In Eq. (29), C should be D. In Eqs. (30a) and (30b), B should be E. In Eq. (31), Q^4 should be Q^2, $\hbar$ should be h, $A_0^{(1)}$ and $A_0^{(2)}$ should be squared, and the $A_0^{(2)}$ factor should be multiplied by 4. Equation (33) should contain the factor $4\sin\gamma/147$ found in Eq. (31). The expression appearing in Eq. (33) was mistakenly divided by $I^2 = \frac{49}{4}$ and the $\sin\gamma$ factor was omitted.

IV. DATA ANALYSIS

There are four fitting parameters which could be used in comparing predictions of Eqs. (18) and (27) to T_1 results. These are the inverse attempt frequency τ_0 which is assumed independent of temperature and pressure, and the three interaction energies J_a, J_b, and J_c which are assumed to have linear dependence on hydrostatic pressure but to be independent of temperature. The fitting process requires Eq. (27) for $1/T_1$, Eq. (18) for $j(\omega)$, the definitions in Eqs. (8)–(10), and the relation $J_p = (J_a + J_c)/2$.

Unfortunately we did not obtain T_1 data close enough to T_C to observe the 3D regime where T_1 is proportional to $(T - T_C)^{1/2}$. Only in this regime would the relaxation results be sensitive to α or equivalently to J_a. Accordingly, we use only the τ_0, J_b, and J_c parameters to fit the T_1 data. To find J_a and its pressure dependence, we use the method of Blinc and Sa Barreto[23] which relies on the slopes dT_C/dp of transition temperature versus pressure both above and below the triple-point pressure. Our method differs from theirs only in that we use the pressure dependences of both J_b and J_c determined from the T_1 fit, whereas they implicitly assume no pressure dependence for J_c.

The fit of T_1 for the parameters and their pressure dependences given below is shown in Fig. 2. The straight 2D regime and curved 1D regime portions of the curves are clearly seen.

The parameters and their pressure dependences found from the T_1 fit and from the T_C versus pressure curve are

$\tau_0 = 2.9 \times 10^{-12}$ sec ,

$J_b/k = 225.7\ \text{K} - (6.85\ \text{K/kbar})p$,

$J_c/k = 3.80\ \text{K} - (0.428\ \text{K/kbar})p$,

$J_a/k = 0.305\ \text{K} - (0.0924\ \text{K/kbar})p$.

From the above fundamental parameters, several derived parameters are calculated and presented below to allow comparison with values of these parameters used by other authors,

$J_p/k = 2.05\ \text{K} - (0.520\ \text{K/kbar})p$,

$J_b/J_p \doteq 110$, $J_c/J_a = 12.5$,

$T_C = 153.9$ K, $T_{C\,2D} = 150.9K$, at 1 bar .

These parameters are compared in Table I with some J_b, J_p, and τ_0 values obtained by other workers.

The triple point at which the transition changes from FE to AFE occurs at 3.30 kbar and 124.6 K from the above parameters. At this point J_a becomes negative, so that the ferroelectrically ordered hydrogen-bonded planes have AFE instead of FE stacking, yielding overall AFE order.

Although we did not make any T_1 measurements in the 3D region above T_C, we did look at the NMR spectrum at 152.4 K and atmospheric pressure. This temperature is between the actual T_C and $T_{C\,2D}$ which is the temperature at which the 2D regime T_1 extrapolates to 0. The NMR spectrum was characteristic of the FE rather than the PE phase, indicating indirectly the presence of the 3D regime with its square-root dependence of T_1 on temperature.

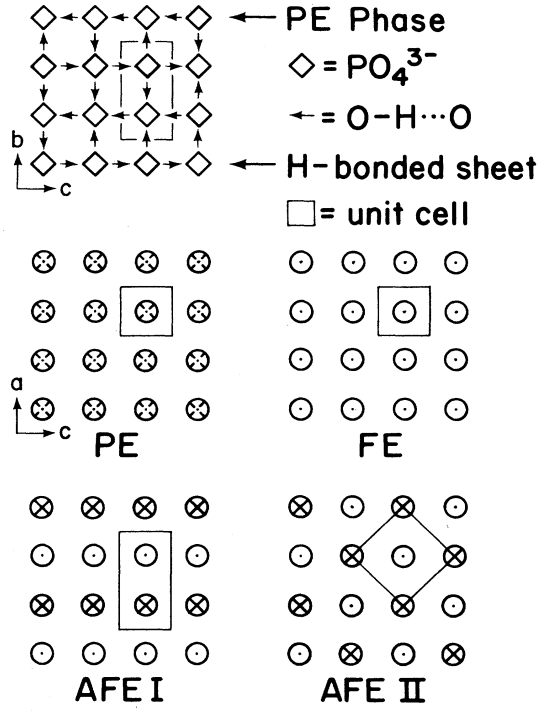

FIG. 3. Ordering of hydrogen bonds in CsH_2PO_4 in paraelectric (PE) phase, ferroelectric (FE) phase, antiferroelectric (AFE I) phase composed of two oppositely polarized planar sublattices, and the postulated antiferroelectric (AFE II) phase composed of two oppositely polarized checkerboard sublattices. Known and postulated (for AFE II phase) unit-cell boundaries are shown also.

V. DISCUSSION

From the above parameters and their pressure dependences, we can predict that if the linear pressure-dependence approximation holds, there will be another triple point at 8.88 kbar and 76.7 K, where J_c should go to 0. Above this pressure, both J_a and J_c would be negative, so that looking along the b axis the chains would order in a checkerboard AFE pattern rather than a sheet pattern. The chain-alignment schemes for the various known and proposed phases appear in Fig. 3. So far, the existence of this second triple point has not been investigated experimentally.

The phase diagram predicted by this linear pressure-dependence assumption appears in Fig. 4. The pressure dependence of T_C is predicted to change sign at this higher triple point, so it should be possible to observe it easily by dielectric means. This figure ends below the

TABLE I. Energy parameters and correlation time from various experiments and theories, for CsH_2PO_4 at atmospheric pressure. Note that some entries differ by factors of 2 or 4 from those appearing in the corresponding references because of differences in definitions of J_b and J_p.

J_b/k (K)	J_p/k (K)	τ_0 (sec)	Method	Ref. no.
225.7	2.05	2.9×10^{-12}	^{133}Cs NMR	This work
234	3.39	1.9×10^{-13}	Dielectric	8
$J_b/J_p = 100$		1.9×10^{-13}	^{31}P chem. shift	10
305	1.8		Dielectric	7
250			Thermal expansion	27
287	1.9		Calorimetic	28
273	3.0	5.7×10^{-14}	Hyper-Raman spec.	29
265.5	3.0		dc dielectric	30
		6.7×10^{-14}	ac dielectric	31
300	3		Dielectric	32
278	2.1		Calorimetric	33

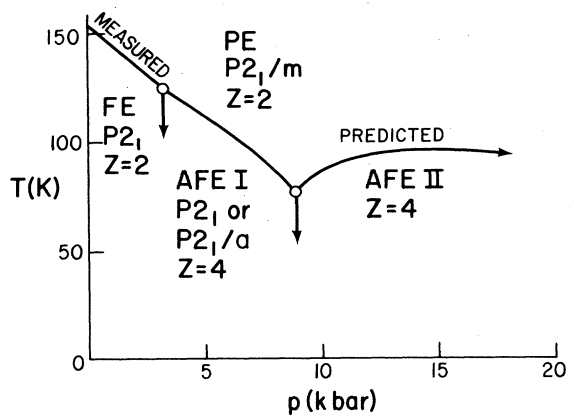

FIG. 4. Known and proposed phase diagram for CsH_2PO_4 at low temperature and moderate hydrostatic pressure, showing monoclinic space groups and number Z of molecules per unit cell. Known phase boundaries are solid lines, proposed boundaries are dashed lines. Phases shown are paraelectric (PE), ferroelectric (FE), planar antiferroelectric (AFE I), and proposed checkerboard antiferroelectric (AFE II).

pressure of 32.9 kbar where the linear extrapolation of J_b goes to 0, because that is too long an extrapolation to be taken seriously.

Additional phase information appears in the work of Rapaport, Clark, and Richter,[24] who presented a high-pressure phase diagram extending to 45 kbar but only down to 0 °C. They show an ill-defined boundary between the PE phase (their phase III) and their phase V, which begins at 11 kbar and 150 °C and which extrapolates approximately to our PE-AFE II phase boundary at the 70 K, 20 kbar point. One possibility is that in their phase V the c-axis hydrogen bonds also become disordered. Their phase I, which occurs above 503 K at 1 bar, was recently shown by Baranov *et al.*[25] to exhibit superionic conductivity. Finally, Baranowski *et al.*[26] reported a transition at 1 bar and 380±1.5 K, in contradiction to the report by Rapaport *et al.* that the PE phase is stable at 1 bar up to 422 K.

We do not attempt a critical evaluation of the various parameters presented in Table I. We simply note that our 1-bar values for J_b and J_p are near the ranges found by other workers.[7,8,10,27–33] Also, the ratio $J_c/J_a=12.5$ at 1 bar is near the value of 10 found by BLTZ. Our large value for τ_0 is troublesome. Perhaps the efg fluctuations are considerably larger than those occurring when a ferroelectric domain reverses, in which case a smaller and more reasonable value of τ_0 would give the correct T_1 magnitudes.

In conclusion, our results are in good accord with the BLTZ theory, and provide a more complete test of that theory than was possible based on the limited atmospheric pressure data of that paper. We have extended the BLTZ theory to show the specific behaviors associated with the 1D, 2D, and 3D fluctuation regions. Based on these results a second triple point where the PE phase meets both planar and checkerboard AFE phases is predicted. We hope that someone will undertake an experimental search for this triple point.

ACKNOWLEDGMENTS

We thank J. T. Wang for his careful growth of CsH_2PO_4 crystals, and S. Žumer, B. Topič, and R. Blinc for helpful discussions concerning their theory. The hospitality of personnel at the Jožef Stefan Institute (Ljubljana, Yugoslavia) and support from the Fulbright Foundation during the time that the results were being analyzed, are acknowledged by one of us (V.H.S.). This work was supported in part by National Science Foundation Grant Nos. DMR-8205280 and DMR-8714487.

*Present address: Ramtron Corporation, 1873 Austin Bluffs Parkway, Colorado Springs, Colorado 80918.

[1]A. Levstik, R. Blinc, P. Kadaba, S. Čižikov, I. Levstik, and C. Filipič, Solid State Commun. **16**, 1339 (1975).
[2]N. Yasuda, M. Okamoto, H. Shimizu, S. Fujimoto, K. Yoshino, and Y. Inuishi, Phys. Rev. Lett. **41**, 1311 (1978).
[3]P. J. Schuele and R. Thomas, Jpn. J. Appl. Phys. **24**, Suppl.. 24-2, 935 (1985).
[4]Y. Iwata, N. Koyano, and I. Shibuya, J. Phys. Soc. Jpn. **49**, 304 (1980).
[5]R. Youngblood, B. C. Frazer, J. Eckert, and G. Shirane, Phys. Rev. B **22**, 228 (1980).
[6]D. Semmingsen, W. D. Ellenson, B. C. Frazer, and G. Shirane, Phys. Rev. Lett. **38**, 1299 (1977).
[7]R. Blinc, B. Žekš, A. Levstik, C. Filipič, J. Slak, M. Burgar, I. Zupančič, L. A. Shuvalov, and A. I. Baranov, Phys. Rev. Lett. **43**, 231 (1979).
[8]E. Kanda, A. Tamaki, and T. Fujimara, J. Phys. C **15**, 3401 (1982).
[9]S. Waplak, V. H. Schmidt, and J. E. Drumheller, Phys. Rev. B **34**, 6532 (1986).
[10]R. Blinc, I. Zupančič, G. Lahajnar, J. Slak, V. Rutar, M. Verbec, and S. Žumer, J. Chem. Phys. **72**, 3626 (1980).
[11]J. Seliger, V. Žagar, and R. Blinc, J. Chem. Phys. **81**, 3247 (1984).
[12]B. Topič, V. Rutar, J. Slak, M. I. Burgar, S. Žumer, and R. Blinc, Phys. Rev. B **21**, 2695 (1980).
[13]R. Blinc, M. Mali, J. Slak, J. Stepišnik, and S. Žumer, J. Chem. Phys. **56**, 3566 (1972).
[14]E. Kanda and T. Fujimara, J. Phys. Soc. Jpn. **43**, 1813 (1977).
[15]R. Blinc, B. Ložar, B. Topič, and S. Žumer, J. Phys. C **16**, 5053 (1983).
[16]P. J. Schuele, Ph.D. thesis, Montana State University, 1988, University Microfilm 88-11056.
[17]P. J. Schuele and V. H. Schmidt, Rev. Sci. Instrum. **31**, 1724 (1982).
[18]M. Suzuki and R. Kubo, J. Phys. Soc. Jpn. **24**, 51 (1968).
[19]D. J. Scalapino, Y. Imry, and P. Pincus, Phys. Rev. B **1**, 2042 (1975).
[20]S. Žumer, Phys. Rev. B **21**, 1298 (1980).
[21]B. C. Frazer, D. Semmingsen, W. D. Ellenson, and G. Shirane, Phys. Rev. B **20**, 2745 (1979).
[22]A. I. Morosov and A. S. Sigov, Ferroelectrics Lett. **2**, 105 (1984).

[23]R. Blinc and F. C. Sa Barreto, J. Chem. Phys. **72**, 6031 (1980).
[24]E. Rapaport, J. B. Clark, and P. W. Richter, J. Solid State Chem. **24**, 423 (1978).
[25]A. I. Baranov, V. P. Khiznichenko, V. A. Sandler, and L. A. Shuvalov, Ferroelectrics **81**, 183 (1988).
[26]B. Baranowski, M. Friesel, and A. Lunden, Z. Naturforsch. **41a**, 981 (1986).
[27]E. Nakamura, K. Abe, and K. Deguchi, J. Phys. Soc. Jpn. **53**, 1614 (1984).
[28]K. Imai, J. Phys. Soc. Jpn. **52**, 3960 (1983).
[29]S. Shin, A. Ishida, T. Yamakami, T. Fujimura, and M. Ishigame, Phys. Rev. B **35**, 4455 (1987).
[30]K. Deguchi, E. Okaue, and E. Nakamura, J. Phys. Soc. Jpn. **51**, 3569 (1982).
[31]K. Deguchi, E. Nakamura, E. Okaue, and N. Aramaki, J. Phys. Soc. Jpn. **51**, 3575 (1982).
[32]S. Watarai and T. Matsubara, Prog. Theor. Phys. **71**, 840 (1984).
[33]E. Kanda, M. Yoshizawa, T. Yamakami, and T. Fujimura, J. Phys. C **15**, 6823 (1982).